Defects as qubits in 3C- and 4H-SiC

L. Gordon, A. Janotti, and C. G. Van de Walle

Phys. Rev. B **92**, 045208 — Published 20 July 2015

DOI: 10.1103/PhysRevB.92.045208

Defects as qubits in 3C- and 4H-SiC

L. Gordon, A. Janotti, and C. G. Van de Walle
Materials Department, University of California, Santa Barbara, CA 93106-5050, USA
(Dated: June 29, 2015)

We employ hybrid density functional calculations to search for defects in different polytypes of SiC that may serve as qubits for quantum computing. We explore the divacancy in 4H- and 3C-SiC, consisting of a carbon vacancy adjacent to a silicon vacancy, and the NV center in 3C-SiC, in which the substitutional N_C sits next to a Si vacancy (N_C-V_{Si}). The calculated excitation and emission energies of the divacancy in 4H-SiC are in excellent agreement with experimental data, and aid in identifying the 4 unique configurations of the divacancy with the 4 distinct zero-phonon lines observed experimentally. For 3C-SiC, we identify the paramagnetic defect that was recently shown to maintain a coherent quantum state up to room temperature as the spin-1 neutral divacancy. Finally, we show that the $(N_C$-$V_{Si})^-$ center in 3C-SiC is highly promising for quantum information science, and we provide guidance for identifying this defect.

It has recently been found that certain point defects in wide-band-gap semiconductors can serve as qubits for quantum computing.[1] These centers are stable in well defined spin states that can be initialized and manipulated at room temperature using optical and microwave excitations, and are responsive to electric and magnetic fields. The prototype of this class of qubits is the NV center in diamond, which is composed of a substitutional N impurity next to a vacancy. In the negative charge state [$(NV)^-$], optical transitions between the S=1 ground state ($^3A_2$) and the ^3E excited state result in luminescence that can be modulated by an external magnetic field.[2] It has also been demonstrated that the $(NV)^-$ center exhibits long spin-coherence times at room temperature.[3] These favorable properties have stimulated a search for analogous defects in materials other than diamond.[4] One obvious candidate material is silicon carbide, a compound that is closely related to diamond in structure and bonding.

SiC is a wide-band-gap semiconductor, available as high-quality large single crystals and epitaxial films,[6] and is the basis for a wide variety of electronic and optoelectronic devices.[7] Recent theoretical work has identified the N_C-V_{Si} center in 4H-SiC as a promising candidate for qubit applications.[4,5] First-principles calculations and experimental measurements have also indicated that the neutral divacancy in 4H-SiC has desirable properties[8–10] (see Fig. 1): photoluminescence, angle-resolved magneto-luminescence, and continuous-wave optically-detected magnetic resonance (ODMR) measurements have demonstrated room-temperature spin control, with spin-coherence properties comparable to those of the NV center in diamond.[10]

There are four symmetry-inequivalent forms of the divacancy in 4H-SiC. Since all have the same local bonding environment and are similarly stable, they coexist in 4H-SiC, and lead to slightly different excitation and emission energies, which potentially poses problems when trying to address individual centers. Furthermore, the charge-neutral divacancy in 4H-SiC is stable only over a limited range of Fermi-level values within the band gap and requires semi-insulating samples. An alternative to 4H-SiC is to use the cubic polytype 3C-SiC, which has the zinc-blende crystal structure and can also be grown as large single crystals and epitaxial films.[11,12]

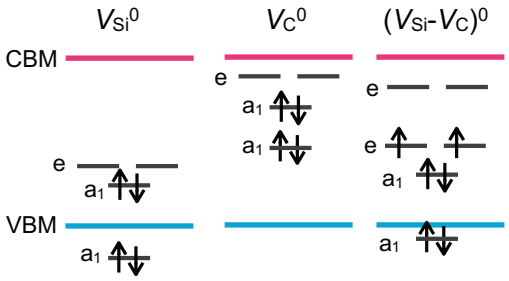

FIG. 1: Schematic single-particle-based electronic structure of the ground state of neutral Si and C vacancies and the neutral divacancy in 4H-SiC. VBM indicates the valence-band maximum and CBM the conduction-band minimum (color online).

The divacancy and NV center are expected to behave similarly in 3C-SiC and 4H-SiC, but the higher symmetry of the 3C polytype eliminates the problem of symmetry-inequivalent configurations. In addition, its smaller band gap (2.36 eV,[20] 0.9 eV smaller than that of 4H-SiC) could potentially be favorable for stabilizing the desired charge states, provided the relevant defect states are not too close to, or resonant with, the valence or conduction bands. A small number of studies have reported on the divacancy in 3C-SiC,[13–15] but detailed information about the stability and electronic and optical properties is lacking, providing the motivation for the present study.

Using first-principles calculations we show that the divacancy in 3C-SiC indeed exhibits similar properties as in 4H-SiC, but has the advantage that the desired charge-neutral vacancy with its S=1 spin state is stable over a range of Fermi levels near the conduction-band minimum (CBM) of 3C-SiC, which is easily achieved by n-type doping. In contrast, the neutral divacancy in 4H-SiC is stable only if the Fermi level is between 0.9 and 2.1 eV above the valence-band maximum (VBM), requiring semi-insulating material with ϵ_F within a specific range, which may be more difficult to achieve in a device.

Our calculations are based on density functional theory

TABLE I: Lattice parameters and band gaps of 4H-SiC and 3C-SiC calculated using the HSE functional. Experimental values[20,21] are listed for comparison.

Material	Property	HSE	Exp.
4H-SiC	a (Å)	3.07	3.07
	c (Å)	10.04	10.05
	E_g (eV)	3.17	3.23
3C-SiC	a (Å)	4.35	4.36
	E_g (eV)	2.24	2.36

(DFT)[16] and the screened hybrid functional developed by Heyd, Scuseria, and Ernzerhof (HSE),[17] as implemented in the VASP code.[18] In the HSE hybrid functional the exchange potential is split into short- and long-range parts, with the range separation determined through an error function with a characteristic screening length of 10 Å. In the short-range region, the exchange potential of Perdew, Burke and Ernzerhof (PBE)[19] is mixed with the non-local Hartree-Fock exchange potential in a ratio of 75:25. The long-range region is described by the PBE functional, and so is the correlation potential. The lattice parameters and band gaps of 3C- and 4H- SiC obtained using HSE along with the experimental values are listed in Table I. We observe excellent agreement between the calculated and experimental values.

To study the properties of the defects, we perform calculations using a 96-atom supercell for 4H-SiC and a 216-atom supercell for 3C-SiC, with a 2×2×2 Monkhorst-Pack k-point mesh for integrations over the Brillouin zone, and a 400 eV cutoff for the plane-wave basis set. The stability of the different charge states for each defect is determined by calculating formation energies.[22] For example, in the case of a divacancy in 4H-SiC, the formation energy for a given charge state of the defect is given by:

$$E^f[(V_{\rm Si}\text{-}V_{\rm C})^q] = E_{\rm tot}[(V_{\rm Si}\text{-}V_{\rm C})^q] - E_{\rm tot}({\rm SiC}) + \mu_{\rm Si} + \mu_{\rm C} + q\cdot\epsilon_F + \Delta^q, \quad (1)$$

where $E_{\rm tot}$(SiC) is the total energy of the pristine 4H-SiC supercell and $E_{\rm tot}[(V_{\rm Si}\text{-}V_{\rm C})^q]$ is the total energy of the supercell containing the defect in charge state q. $\mu_{\rm Si}$ and $\mu_{\rm C}$ are the chemical potentials of Si and C referenced to the total energy per atom of bulk Si and diamond, respectively, and can vary over a range limited by the enthalpy of formation of SiC. The Si-rich limit is set by $\mu_{\rm Si}$=$E_{\rm tot}$(Si) and thus $\mu_{\rm C}$=$E_{\rm tot}$(C)+ΔH_f(SiC), and the C-rich limit by $\mu_{\rm Si}$=$E_{\rm tot}$(Si)+ΔH_f(SiC) and $\mu_{\rm C}$=$E_{\rm tot}$(C), where ΔH_f(SiC) is the enthalpy of formation of 4H-SiC. In the case of NV centers, we considered Si_3N_4 as the solubility-limiting phase, allowing us to set an upper bound on the N chemical potential. ϵ_F is the Fermi level, which is referenced to the VBM. Δ^q is the correction term to align the electrostatic potential in the perfect bulk and defect supercells and to account for finite-cell size effects on the total energies of charged defects.[23,24]

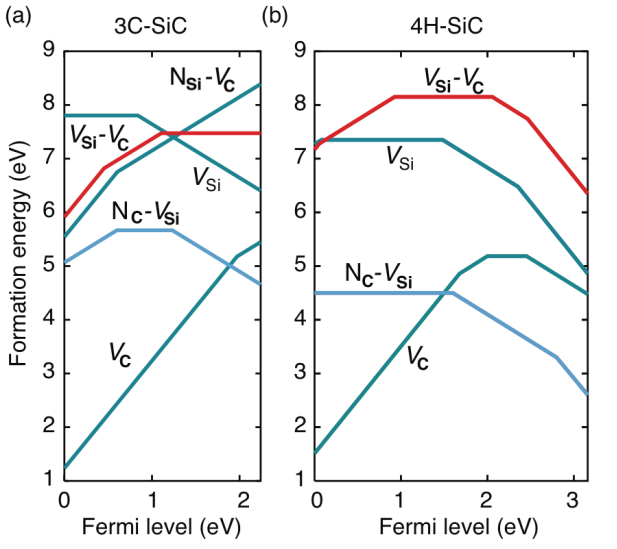

FIG. 2: Formation energy as a function of Fermi level for single vacancies ($V_{\rm C}$ and $V_{\rm Si}$), divacancy ($V_{\rm C}$-$V_{\rm Si}$), and NV centers in 3C- and 4H-SiC, under C-rich conditions (color online).

In Figure 1 we show formation energies for single vacancies, divacancies and NV centers in 4H-SiC and 3C-SiC in the C-rich limit. The slopes indicate the stable charge state for a given position of the Fermi level [see Eq. (1)], and the kinks represent the charge-state transition levels (q/q'), i.e., the Fermi-level position below which the defect is stable in charge state q and above which it is stable in charge state q'.[22] Note that different charge states for the same defect involve distinct local lattice relaxations. Proper identification and occupation of the defect states for various charge states was facilitated by the small dispersion of the defect-related states in the gap. The symmetry was analyzed by inspecting the atomic positions surrounding the defect and the degeneracy of the defect-related states at the Γ point.

The formation energies for the divacancies and NV centers are very high and imply that the concentration of these defects, which is proportional to e^{-E_f/k_BT}, are expected to be extremely low under equilibrium conditions. However, as previously observed by Torpo *et al.*,[13] the binding energy of the divacancy is very high, around 3-4 eV for Fermi level positions near the middle of the band gap. Since SiC is grown at temperatures exceeding 1600 °C,[11] single vacancies that are formed during growth will be highly mobile, tending to meet and form complexes. Divacancies can also be intentionally created through implantation and annealing.[15]

Perhaps more relevant than the absolute formation energies, for the purposes of the present study, are the positions of the transition levels and the range of Fermi-level values over which defects are stable in a given charge state. For instance, the divacancy in 4H-SiC is predicted to be stable in the neutral charge state for Fermi-level values between 0.9 eV and 2.1 eV, requiring 4H-SiC to be semi-insulating. This is consistent with experimental

observations.[10] In the case of 3C-SiC, we find that the neutral divacancy is a S=1 triplet and is stable for all Fermi levels above 1.0 eV. In addition, we find that the negative N_C-V_{Si} center also forms a spin triplet and is stable for all Fermi levels above 1.3 eV.

Further insight into the stability of the different charge states of a given defect is provided by inspecting the spectrum and occupancy of the defect-related single-particle states in the gap. Isolated vacancies in SiC introduce levels that are derived from the four dangling bonds of the surrounding atoms. In 4H-SiC these dangling bonds combine into two symmetric one-electron states (a_1) and a doubly degenerate e state. In the case of a Si vacancy, the states in the gap are derived from C dangling bonds and lie close to the valence band; for the C vacancy, the states are derived from Si dangling bonds and lie closer to the conduction band, as shown in Fig. 1. In the case of divacancies, there are six dangling bonds, which combine into two a_1 and two e states. The lower a_1 and lower e states are derived from the C dangling bonds and the higher a_1 and e states are derived from the Si dangling bonds. In the neutral charge state four electrons occupy the a_1 states, and two electrons occupy the lower degenerate e level. Following Hund's rule, the electrons in the e level have parallel spin. The level structure of the NV center can be derived in a similar manner.[4]

A key difference between the divacancy in 3C-SiC and 4H-SiC is that the e states associated with the Si dangling bonds lie above the CBM due to the smaller band gap of 3C-SiC, meaning that it is not possible to occupy them with electrons. As a result, negative charge states cannot be stabilized and the neutral charge state is stable for all Fermi levels in the upper part of the gap. As such, this will be the stable charge state in n-type 3C-SiC. In 4H-SiC, on the other hand, the Si-dangling-bond-associated e states lie in the gap, and the (0/–) and (–/–2) transition levels occur at 1.2 and 0.7 eV below the CBM. Similarly, for the N_C-V_{Si} center the empty spin-down e state, derived from Si dangling bonds, lies above the CBM in 3C-SiC but within the gap in 4H-SiC. As a consequence, the –2 charge state cannot be stabilized for the N_C-V_{Si} center in 3C-SiC, but does occur in 4H-SiC, with a (–/–2) transition level at 0.4 eV below the CBM.

In analogy with the NV center in diamond, the centers that are promising as qubits in SiC are those that have an S=1 ground state that can be optically manipulated by exciting an electron from the highest a_1 state to one of the e states, as shown in Fig. 1. This occurs for the neutral divacancy $(V_C$-$V_{Si})^0$ and the negatively charged $(N_C$-$V_{Si})^-$ center. The peak excitation and emission energies can be calculated by constraining the occupation and taking total-energy differences between the excited and ground-state configurations, allowing the determination of a configuration coordinate diagram.[25] The calculated configuration diagrams are shown in Fig. 3 and the energies of the optical transitions are listed in Table II.

In 4H-SiC, there are four different forms of the divacancy: the kk and hh forms of the axial divacancy (k stands for quasi-cubic position and h for quasihexagonal), and the kh and hk forms of the basal divacancy.[26] We have calculated absorption, emission and zero-phonon line energies for each defect, as shown in Fig. 3 and Table II.

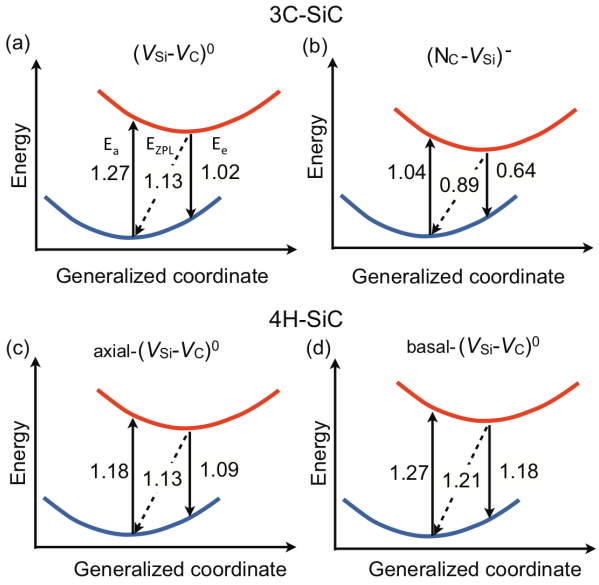

FIG. 3: Configuration coordinate diagrams for (a) the axial (hh) and (b) the basal (hk) divacancies in 4H-SiC, and (c) the divacancy and (d) the NV center in 3C-SiC. All values for absorption (E_a), emission (E_e), and zero-phonon line (E_{ZPL}) energies are in eV (color online).

TABLE II: Calculated absorption, zero-phonon line (ZPL) and emission energies for all divacancies in 4H-SiC, and for the divacancy and N_C-V_{Si} center in 3C-SiC. Experimental values[10,14] for E_{ZPL} are shown where available.

Polytype	Defect	E_a	E_{ZPL}	E_e	E_{ZPL}^{exp}
4H	V_{Si}-V_C (hh)	1.18	1.13	1.09	1.094
4H	V_{Si}-V_C (kk)	1.19	1.14	1.10	1.095
4H	V_{Si}-V_C (hk)	1.27	1.21	1.18	1.120
4H	V_{Si}-V_C (kh)	1.29	1.24	1.21	1.150
3C	V_{Si}-V_C	1.27	1.13	1.02	1.121
3C	N_C-V_{Si}	1.04	0.89	0.64	

The results for ZPLs agree extremely well with experiment[10] and previous calculations for clusters,[9,27] to within 0.1 eV accuracy in all cases. The axial divacancy ZPL energies are experimentally measured to be within 0.001 eV of one another, consistent with our calculation of a small 0.01 eV difference between the two forms of the axial divacancy. Similarly, the basal divacancy ZPL energies are measured to be 0.03 eV apart, in complete agreement with our calculations, which find a 0.03 eV difference between the hk and kh basal divacancies..[10] Based on our calculations, we can assign the hk and kh basal divacancies to the experimental ZPL energies at 1.12 eV and 1.15 eV, respectively. We can also tentatively assign the hh and kk axial divacancies to the experimental lines

at 1.094 eV and 1.095 eV, although the energy difference is smaller than the error bar on the calculations.

In the case of the neutral divacancy in 3C-SiC [Fig. 3(c)] we find an excitation energy of 1.27 eV, an emission peak at 1.02 eV, and the ZPL at 1.13 eV. The divacancy has not yet been conclusively experimentally identified in 3C-SiC. However, an optically detected magnetic resonance study of 3C-SiC by Son *et al.*[14] reported an S=1 defect with trigonal symmetry and a measured ZPL of 1.121 eV. The authors hypothesized that this peak was due to a complex involving a silicon vacancy and another intrinsic defect. We think it highly likely that this defect is in fact the S=1 neutral divacancy. Recent experimental work[15] has confirmed the existence of this spin-1 defect in 3C-SiC with a peak at 1.121 eV, and shown that it is coherent and optically addressable up to room temperature.

The $(N_C$-$V_{Si})^-$ center in 4H-SiC has been previously suggested[4] as a potential NV-like qubit. Our calculations show that the $(N_C$-$V_{Si})^-$ center in the 3C polytype is also highly promising as a qubit: it is a spin triplet in the ground and excited states, with emission and absorption peaks in the infrared [Fig. 3(d)]. Infrared luminescence has rarely been used to study NV-like point defects, possibly because the luminescence in that wavelength region tends to be dominated by transition-metal and rare-earth impurities.[28] Vanadium and erbium, in particular, are common impurities in as-grown SiC, and sharply peaked emission spectra between 0.8 and 0.95 eV are observed,[29] arising from intra-d-shell and intra-f-shell transitions. Our calculations yield a binding energy of 2.0 eV for the $(N_C$-$V_{Si})^-$ center in 3C-SiC, consistent with the value obtained in 4H-SiC by Weber *et al.*.[30] We therefore expect nitrogen-doped SiC with a substantial concentration of V_{Si}, obtained via high-temperature growth or implantation/irradiation, to contain a substantial concentration of $(N_C$-$V_{Si})^-$ centers. Specific formation mechanisms of N_C-V_{Si} centers and their concentrations in 3C-SiC have been proposed based on calculated migration barriers and formation energies in Refs.31 and32. These centers should exhibit ZPL energies at around 0.89 eV for 3C-SiC, and 1.09 eV[30] for 4H-SiC.

In summary, we have used first-principles calculations to study properties of various point defects in 4H-SiC and 3C-SiC that can serve as qubits, reporting their formation energies, transition levels, and optical transition energies. Our calculations for the divacancy in 4H-SiC allow us to assign the experimentally observed ZPLs[10] to specific microscopic vacancy configurations. Our results for the neutral divacancy in 3C-SiC suggest that this is the defect that has been observed to give rise to a spin-1 center with a ZPL peak at 1.121 eV.[14,15] We also find that the $(N_C$-$V_{Si})^-$ center in 3C-SiC is highly promising for qubit applications. Unlike the situation in 4H-SiC, where semi-insulating material is needed with the Fermi-level within a specific range, the desired S=1 state of the $(V_C$-$V_{Si})^0$ and the $(N_C$-$V_{Si})^-$ centers is stable in n-type-doped 3C-SiC, which should make experimental observation and control more straightforward than in the 4H polytype.

We are grateful to J. B. Varley, W. Koehl, G. Calusine and D. D. Awschalom for useful discussions. Computational resources were provided by the Center for Scientific Computing at the CNSI and MRL (an NSF MRSEC, DMR-1121053) (NSF CNS-0960316) and by XSEDE, NSF grant ACI-1053575 (DMR070072N).

[1] P. Neumann, N. Mizuochi, F. Rempp, P. Hemmer, H. Watanabe, S. Yamasaki, V. Jacques, T. Gaebel, F. Jelezko, J. Wrachtrup, Science **320**, 1326 (2008).
[2] N. B. Manson, J. P. Harrison and M. J. Sellars, Phys. Rev. B **74**, 104303 (2006).
[3] G. Balasubramanian, P. Neumann, D. Twitchen, M. Markhan, R. Kolesov, N. Mizuochi, J. Isoya, J. Achard, J. Beck, J. Tissler, V. Jacques, P. R. Hemmer, F. Jelezko, J. Wrachthrup, Nat. Mater. **8**, 383 (2009).
[4] J. R. Weber, W. F. Koehl, J. B. Varley, A. Janotti, B. B. Buckley, C. G. Van de Walle, D. D. Awschalom, Proc. Nat. Acad. Sci. **107**, 8513 (2010).
[5] K. Szász, V. Ivády, E. Janzén, and A. Gali, Mater. Sci. Forum **778-780**,499 (2014).
[6] A. Powell, J. Jenny, S. Muller, H. McD. Hobgood, V. Tsvetkov, R. Lenoard, C. Carter, Int. J. High Speed Electron. Syst. **16**, 751 (2006).
[7] C. M. Zetterling (ed.), *Process Technology for Silicon Carbide Devices* (2002), INSPEC, The Institution of Electrical Engineers, London, United Kingdom.
[8] N. T. Son, P. Carlsson, J. ul Hassan, E. Janzén, T. Umeda, J. Isoya, A. Gali, M. Bockstedte, N. Morishita, T. Ohshima, H. Itoh, Phys. Rev. Lett. **96**, 055501 (2006).
[9] A. Gali, Phys. Stat. Solidi B **248**, 1337 (2011).
[10] W. Koehl, B. B. Buckley, F. J. Heremans, G. Calusine, D. D. Awschalom, Nature **479**, 84 (2011).
[11] A. J. Steckl, J. Devrajan, S. Tlali, H. E. Jackson, C. Tran, S. N. Gorin and L. M. Ivanova, Appl. Phys. Lett. **69**, 3824 (1996).
[12] C. A. Zorman, A.J. Fleischman, A.S. Dewa, M. Mehregany, C. Jacob, S. Nishino, and P. Pirouz, J. Appl. Phys. **78**, 5136 (1995).
[13] L. Torpo, T. E. M. Staab and R. M. Nieminen, Phys. Rev. B. **65** 8 085202 (2002).
[14] N. T. Son, E. Sörman, W. M. Chen, C. Hallin, O. Kordina, B. Moneman, E. Janzen, J. L. Lindström, Phys. Rev. B **55** 2863 (1997).
[15] A. L. Falk, B. B. Buckley, G. Calusine, W. F. Koehl, V. V. Dobrovitski, A. Politi, C. A. Zorman, P. X.-L. Feng, D. D. Awschalom, Nature Comm., **4** 1819 (2013).
[16] P. Hohenberg and W. Kohn, Phys. Rev. **136**, B864 (1964); W. Kohn, L. J. Sham, Phys. Rev. **140**, A1133 (1965).
[17] J. Heyd, G. E. Scuseria, and M. Ernzerhof, J. Chem. Phys. **118**, 8207 (2003); **124**, 219906 (2006).
[18] G. Kresse and J. Furthmüller, Phys. Rev. B **54**, 11169 (1996).

[19] J. P. Perdew, K. Burke, and M. Ernzerhof, Phys. Rev. Lett. **77**, 3865 (1996).
[20] Y. Goldberg, M.E. Levinshtein, S.L. Rumyantsev, *Properties of Advanced Semiconductor Materials*, edited by M. E. Levinshtein, S. L. Rumyantsev, and M. S. Shu, Wiley, New York, p. 93-148 (2001).
[21] A. Taylor and R. M. Jones, in *Silicon Carbide - A High Temperature Semiconductor*, edited by J. R. O'Connor and J.R., Smiltens, Pergamon Press, Oxford, 147 (1960).
[22] C. Freysoldt, B. Grabowski, T. Hickel, G. Kresse, A. Janotti, J. Neugebauer, and C. G. Van de Walle, Rev. Mod. Phys. **86**, 253 (2014).
[23] C. Freysoldt, J. Neugebauer, and C. G. Van de Walle, Phys. Rev. Lett. **102**, 016402 (2009).
[24] C. Freysoldt, J. Neugebauer, and C. G. Van de Walle, Phys. Status Solidi B **248**, 1067 (2011).
[25] A. M. Stoneham, Theory of Defects in Solids (Oxford University Press, 1975).
[26] L. Gordon, J. R. Weber, J. B. Varley, A. Janotti, D. D. Awschalom and C G. Van de Walle, MRS Bulletin, **38**, 10 (2013).
[27] A. Gali, J. Mater. Res. **27**, 897 (2012).
[28] J. Schneider, H. D. Mller, K. Maier, W. Wilkening, F. Fuchs, A. Dornen, S. Leibenzeder and R. Stein, Appl. Phys. Lett. **56**, 1184 (1990).
[29] R. A. Babunts, V. A. Vetrov, I. V. Ilin, E. N. Mokhov, N. G. Romanov, V. A. Khramtsov, and P. G. Baranov, Physics of the Solid State, **56**, 1184 (1999).
[30] J. R. Weber, W. F. Koehl, J. B. Varley, A. Janotti, B. B. Buckley, C. G. Van de Walle and D. D. Awschalom, J. Appl. Phys. **109**, 102417 (2011).
[31] U. Gerstmann, E. Rauls, Th. Frauenheim, and H. Overhof, Phys. Rev. B **67**, 205202 (2003).
[32] M. Bockstedte, A. Mattausch, and O. Pankratov, Appl. Phys. Lett. **85**, 58 (2004).